CFAR TARGET DETECTION IN TREE SCATTERING INTERFERENCE

Anshul Sharma and Randolph L. Moses
Department of Electrical Engineering,
The Ohio State University, Columbus, OH 43210

ABSTRACT

We have developed linear subspace detectors that detect targets in a background of both noise and tree responses. We consider the background clutter as stochastic noise, and we model the tree responses as a deterministic signal with unknown amplitude and unknown parameters. We develop a family of target detectors based on different assumptions on what is known about the taget and the tree families, and what is known about the noise statistics. We compare performance under several scenarios.

1 INTRODUCTION

Ultra-WideBand (UWB) radar sensors show promise for enhancing the situational awareness of army Brigades. UWB radars have been proposed for surveillance and target acquisition in high-clutter environments such as heavy foliage, providing enhanced situational understanding. UWB radar systems also have application in mine detection to provide improved situational awareness and improved soldier and Brigade safety. Thus, development of UWB technology is aimed at providing a more robust sensor suite with higher capabilities than is currently available to the Brigade. In this paper we develop improved target acquisition algorithms for UWB systems operating in severe clutter environments.

Constant False Alarm Rate (CFAR) detectors are often employed for object detection from measured radar imagery. CFAR detectors attempt to find points of interest whose amplitude or energy is large in comparison to local scatttered energy in the region of the point. As an example, a two-parameter Gaussian CFAR detector estimates the mean and variance of pixels in the neighborhood of a point under consideration, and tests if the amplitude of that point is more than c standard deviations from the mean, where c is a user-selected constant that controls the false alarm rate.

For object detection from Ultra-WideBand (UWB) radar imagery, alternatives to Gaussian CFAR detection are often sought. There are a number of reasons for this. First, the clutter in high resolution radar imagery obtained at low frequencies, such as the UWB imagery measured by the ARL UWB sensor, is not well-modeled as Gaussian noise in many cases. Some studies have suggested that the clutter is more accurately modeled as a heavy-tailed distribution, such as a K-distribution or an α-stable random process. CFAR detectors that employ these models have been developed [1, 2]. For imagery in forested areas, CFAR detectors give high false alarm rates for a given desired probability of detection of objects of interest. The reason for this is that tree trunk scattering appears as a locally bright region, and passes the CFAR detection test. CFAR detectors that assume a heavy-tailed distribution are only marginally helpful in reducing the false alarm rate.

In this paper we take a different approach to the detector problem. We assume the radar signal is a combination of objects of interest, of clutter modeled as a random "noise", and of interference terms of unknown amplitude. The interference will be used to model tree scattering. This signal model has been used in multi-user communication applications [3] as well as other detection and estimation applications in the presence of structured interference [4, 5].

We assume the tree scattering is dominated by a signal structure that lies in a low-dimensional subspace of the measured data. Different assumptions can be made about what is known or unknown about tree

Prepared through collaborative participation in the Advanced Sensors Consortium sponsored by the U.S. Army Research Laboratory under the Federated Laboratory Program, Cooperative Agreement DAAL01-96-2-0001. The U.S. Government is authorized to reproduce and distribute reprints for Government purposes notwithstanding any copyright notation thereon.

scattering, leading to subspaces of different dimension. At one extreme, for example, we can take a Geometric Theory of Diffraction (GTD) approximation to tree scattering, and arrive at a one-dimensional interference subspace. At the other extreme we can assume the interference class has an arbitrary isotropic scattering response. Between these two extremes lie the cases in which one has partial knowledge of tree scattering, such as might be known from low-frequency tree scattering predictions.

The detection problem considered in this paper has some relationship with detection of anisotropic scattering by subaperture processing of radar imagery data [6, 7, 8]. Subaperture processing can be considered a special case in which one assumes the interference term is isotropic. Our approach provides some advantages and flexibility: we can incorporate as much or little structured knowledge of both the interference term and the desired signal term to improve detection performance, and we have explicit expressions for the detectors and detection performance using the subspace-based approach. By incorporating partial knowledge of the signal and interference, we improve detection performance.

2 Signal Model

We assume a radar measurement vector Y of dimension $K \times 1$ is given. The measurement can be thought of as a vectorized version of a radar image chip about a candidate point of interest. The signal model we assume is

$$Y = H\theta_d + S\theta_t + \sigma N \qquad (1)$$

where H is a $K \times p$ matrix whose columns span the desired signal subspace and S is a $K \times t$ matrix whose columns span the interference signal subspace. The matrices H and S encode partial knowledge of the signal and interference, respectively. The vectors θ_d and θ_t are unknown amplitudes for the signal and interference, and the vectors $H\theta_d$ and $S\theta_t$ are the $K \times 1$ signal and interference components of Y, respectively. The vector N is a $K \times 1$ vector of noise, which is modeled as zero mean Gaussian noise with covariance R. We assume both H and S are known, but θ_d and θ_t are completely unknown; in this way we encode partial knowledge of the signal and interference components.

3 Detector Structures

The signal detection problem can be formulated as the following hypothesis testing problem:

$$\begin{aligned} H_0 : Y &= S\theta_t + \sigma N && (2) \\ H_1 : Y &= H\theta_d + S\theta_t + \sigma N && (3) \end{aligned}$$

Thus, under H_0 the signal is absent, or $\theta_d = 0$, whereas under H_1 we test $\theta_d \neq 0$. We will further assume that the noise covariance $R = \sigma^2 I$, although extensions to general R are straightforward.

Two GLRT detector structures are analyzed for the cases of known σ and unknown σ.

Case 1 : Known σ When the noise variance is known, the decision rule is given by

$$L_1(Y) = \underset{\mathrm{H}_0}{\overset{\mathrm{H}_1}{\gtrless}} \eta_1 \qquad (4)$$

where

$$L_1(Y) = \frac{Y^T P_s^+ P_G P_s^+ Y}{\sigma^2} \qquad (5)$$

Here, the $K \times K$ matrix $P_s = S(S^T S)^{-1} S^T$ is the projection operation onto the interference subspace $\langle S \rangle \stackrel{\triangle}{=} \text{span}(S)$, and $P_s^+ = I - P_s$ is its orthogonal complement. Similarly, $P_G = H(H^T H)^{-1} H^T$ and $P_G^+ = I - P_G$ project onto and orthogonally to the signal subspace $\langle H \rangle$. The threshold η_1 is selected by the user, and is usually chosen to specify a desired false alarm rate for the detector.

The likelihood ratio statistic is distributed as a chi-squared distribution:

$$\begin{aligned} L_1(Y) &\sim \chi_p^2(0) \text{ under } H_0 && (6) \\ L_1(Y) &\sim \chi_p^2(\lambda^2) \text{ under } H_1 && (7) \end{aligned}$$

where p is the signal subspace dimension and

$$\lambda^2 = \frac{\mu^2}{\sigma^2}(H\theta_d)^T P_s^+ (H\theta_d) \tag{8}$$

is the effective signal-to-noise ratio (SNR). Equations 6 and 7 give an analytical expression for the performance of the detector; in particular, equation 6 can be used to determine the threshold η_1 needed for a given false alarm rate.

Case 2 : Unknown σ When σ^2 is unknown, it is estimated (to within a known constant) by $Y^T P_s^+ P_G^+ P_s^+ Y$. This estimate is the variance estimate obtained by projecting Y to the null space of $\langle H \cup S \rangle$. In this case, the resulting decision rule is given by

$$L_2(Y) \underset{\mathrm{H}_0}{\overset{\mathrm{H}_1}{\gtrless}} \eta_2 \tag{9}$$

where

$$L_2(Y) = \frac{Y^T P_s^+ P_G P_s^+ Y}{Y^T P_s^+ P_G^+ P_s^+ Y} \tag{10}$$

This likelihood ratio statistic is F-distributed:

$$L_2(Y) \sim F_{p,k-(p+t)}(0) \text{ under } H_0 \tag{11}$$

$$L_2(Y) \sim F_{p,k-(p+t)}(\lambda^2) \text{ under } H_1 \tag{12}$$

where

$$\lambda^2 = \frac{\mu^2}{\sigma^2}(H\theta_d)^T P_s^+ (H\theta_d) \tag{13}$$

is the effective SNR in this case. Note that the likelihood ratio depends on the dimensions of the signal and interference subspaces in this case. Similarly to Case 1, equations 11 and 12 give an analytical expression for the performance of the detector, and equation 11 can be used to determine the threshold η_2 needed for a given false alarm rate.

3.1 Properties of the Detectors The above detectors are GLRT detectors, which in general are not optimal. However, these two detectors can be shown to be optimal detectors under the class of invariant detectors that correspond to the unknown parameters [5, 4]. In particular,

1. The tests are Uniformly Most Powerful(UMP), as the test-statistics' distributions are monotone in the non-centrality parameter.
2. The test statistics are invaiant to any translation of the received vector (this includes scaling and rotation) in the interference subspace, $\langle S \rangle$.
3. The test-statistics are also invariant to scaling under rotations in the subspace orthogonal to the interference subspace $\langle S \rangle$.
4. For Case 2, the test-statistic is also invariant to the scaling of Y, because it utilizes the angle which Y makes with the signal subspace, $\langle H \rangle$, after it has been projected orthogonal to $\langle S \rangle$.

4 Performance Analysis

In this section we evaluate the performance of the detectors synthetically generated radar-data using the scattering models in [9]. The signal subspace, $\langle H \rangle$, is the space of all dihedral images, for a quantized set of values of the dihedral length L and orientation angle ϕ_0. The images are converted into vectors by stacking pixel values into columns. An SVD analysis of all these vectors yields the eigenvectors and the corresponding singular values for this subspace. All the image-chips are of size 33x33 (hence K = 1089). The dimension of H used is varied in the experiments. If one were looking for a single dihedral length and orientation, p would be equal to one. In the examples, p is varied from 10 to 55, where $p = 55$ corresponds to 90% of the total energy in the subspace containing all the quantized dihedrals we considered. The interference subspace, $\langle S \rangle$, consists of a tree image generated by using the simple model, $(T(f, \phi) = A\sqrt{f})$, for the tree response in the frequency domain. For this model, the dimension of $\langle S \rangle$, is $t = 1$. We have also used higher interference dimensions using an SVD analysis of available low frequency scattering predictions of trees; the results are similar to those presented. The received data vector is generated by adding together vectors in each of the two subspaces, and adding white Gaussian noise to the result.

Figure 1 shows performance as a function of SNR, for various values of p (p is the dimension of $\langle H \rangle$). Performance is measured as probability of detection (P_d) of a desired scattering center for a probability false alarm fixed at $P_{fa} = 0.01$. From the plot, we observe that the performance improves as p decreases - this is because as p increases the class of desired signals increases, and noise rejection is lower. We thus observe a trade-off between better modeling of $\langle H \rangle$(large p) and better performance (small p). Also, we see very little difference between the performance of the two detectors. This is because of the large dimension of the image-chip, yielding an extremely accurate estimate for σ in case of the second detector.

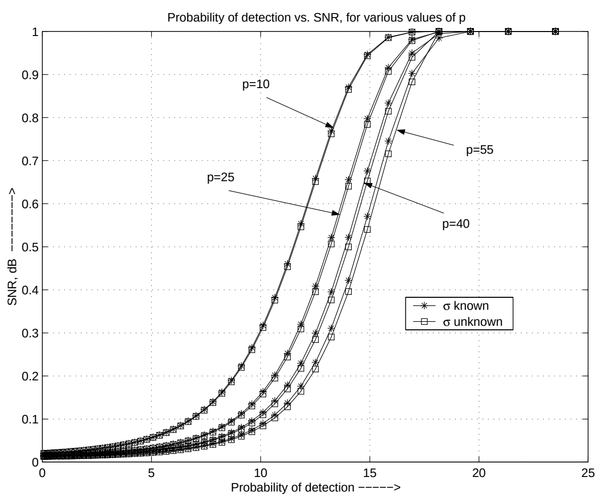

Figure 1: Probability of Detection for Dihedrals as a function of SNR. Here, $P_{fa} = 0.01$ and p represents the dimension of the desired signal subspace.

Figure 2 shows the ROC curve for the two detectors, for various values of p, when the signal-to-noise ratio is fixed at 10 dB. Again, a similar behavior is observed with respect to p.

5 Future Directions

We are currently applying these detectors to measured UWB SAR data collected by ARL. Our goal is to evaluate the performance of the detectors on measured data. We are also currently investigating the the val-

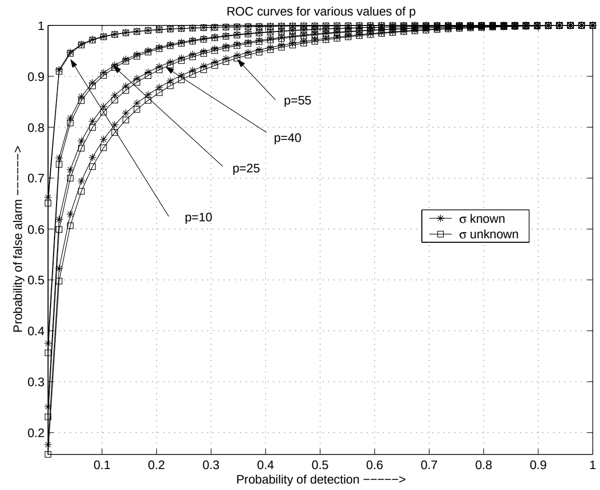

Figure 2: ROC curve for subspace detectors when SNR=10 dB.

ues of SNR and image-chip sizes which would be meaningful for measured data.

6 References

[1] R. L. Dilsavor and R. L. Moses, "Fully polarimetric GLRT for detecting targets with unknown amplitude, phase, and tilt angle in terrain clutter," in *Proc. SPIE International Symposium on Automatic Object Recognition IV*, vol. 2234, (Orlando, FL), pp. 14–25, April 4–8, 1994.

[2] A. Banerjee, P. Burlina, R. Chellappa, and R. Kapoor, "Adaptive segmentation and target detection in foliage penetrating SAR image," *IEEE Trans. on Image Processing*. (to appear).

[3] S. Verdu, *Multiuser Detection*. Cambridge University Press, 1998.

[4] R. Beherens and L. L. Scharf, "Signal processing applications of oblique projection operators," *IEEE Trans. on Signal Processing*, pp. 1413–1423, June 1994.

[5] L. L. Scharf and B. Friedlander, "Matched subspace detectors," *IEEE Trans. on Signal Processing*, pp. 2146–2157, August 1994.

[6] M. R. Allen and L. E. Hoff, "Wide-angle wideband sar matched filter image formation for enhanced detection performace," in *Algorithms for*

Synthetic Aperture Radar Imagery, vol. 2230, (Orlando FL), pp. 302–314, SPIE, April 1994.

[7] J. D. Gorman and J. A. Marble, “Feature based discrimination in UWB SAR,” in *Proceedings of the 2nd Annual Fedlab Symposium*, (College Park, MD), pp. 132–136, February 2–6, 1998.

[8] J. McClellan and R. Rau, “Aspect angle information of targets in UWB SAR iages and new post processing techniques,” in *Proc. 2nd Annual Fedlab Symposium*, (College Park, MD), pp. 127–131, February 2–6, 1998.

[9] E. Ertin, “Performance analysis of anisotropic scattering center detection,” Master’s thesis, The Ohio State University, 1997.